The X-ray Remnant of SN1987A

David N. Burrows ¹ , Eli Michael ² , Una Hwang ³ , Richard McCray ² , Roger A. Chevalier ⁴
Robert Petre ³ , Gordon P. Garmire ¹ , Stephen S. Holt ³ , John A. Nousek ¹

Received ______; accepted _____

 $^{^1\}mathrm{Department}$ of Astronomy & Astrophysics, Penn State University, University Park, PA 16802; burrows@astro.psu.edu

²JILA, University of Colorado, Boulder, CO 80309-0440

³NASA/Goddard Space Flight Center, Greenbelt, MD 20771

⁴Dept. of Astronomy, University of Virginia, P.O. Box 3818, Charlottesville, VA 22903

ABSTRACT

We present high resolution *Chandra* observations of the remnant of SN1987A in the Large Magellanic Cloud. The high angular resolution of the *Chandra X-ray Observatory (CXO)* permits us to resolve the X-ray remnant. We find that the remnant is shell-like in morphology, with X-ray peaks associated with some of the optical hot spots seen in HST images. The X-ray light curve has departed from the linear flux increase observed by ROSAT, with a 0.5-2.0 keV luminosity of 1.5×10^{35} erg/s in January 2000. We set an upper limit of 2.3×10^{34} ergs/s on the luminosity of any embedded central source (0.5 - 2 keV). We also present a high resolution spectrum, showing that the X-ray emission is thermal in origin and is dominated by highly ionized species of O, Ne, Mg, and Si.

1. INTRODUCTION

Supernova 1987A (SN1987A) in the Large Magellanic Cloud was the first supernova explosion visible to the naked eye in nearly 400 years. Because it is located in the nearest galaxy, it provides an unprecedented opportunity to study the early evolution of a supernova remnant (SNR) at a known distance (50 kpc; Andreani et al. 1987) with modern ground-and space-based astronomical instruments. As a result, it has been studied across the entire electromagnetic spectrum, and is the only SN explosion from which a neutrino burst has been detected (Koshiba et al. 1987), confirming our theoretical models of stellar collapse. SN1987A is also the only remnant for which the stellar type of the progenitor star is known from pre-explosion observations: the progenitor was the blue supergiant Sanduleak -69°202, a type B3 I star (Kirshner et al. 1987; Sonneborn, Altner, & Kirshner 1987).

The optical remnant has been studied intensively, both with ground-based instruments and with the HST. HST images show a bright elliptical ring $(1.7 \times 1.2 \text{ arcseconds})$ surrounding the optical remnant. This inner ring has been interpreted as a ring of high-density material in the equatorial plane of the progenitor, caused by the impact of the high velocity stellar wind of the blue supergiant progenitor with its earlier, slower red giant wind, and ionized by the UV flash from the supernova explosion 13 years ago (Burrows et al. 1995).

In recent years, HST observations of SN1987A have revealed a gradually brightening "hot spot" on the inner ring at a position angle of 29 degrees (Garnavich *et al.* 2000). This hot spot has been interpreted as evidence of shock heating at the point of first contact of the supernova blast wave with the relatively dense ($n \sim 10^4 \text{ cm}^{-3}$) inner ring (Michael *et al.* 2000). When the shock front engulfs the remainder of the inner ring, the remnant is expected to brighten by as much as three orders of magnitude at optical, UV, and X-ray wavelengths (Luo, McCray, & Slavin 1994; Borkowski, Blondin, & McCray 1997b). In

the past several months, HST observations have shown that at least four new optical hot spots have appeared along the inner eastern edge of the inner ring (Bouchet *et al.* 2000; Lawrence *et al.* 2000; Maran, Pun, & Sonneborn 2000; Garnavich, Kirshner, & Challis 2000), providing further evidence that this event is well underway. A recent HST image of SN1987A is shown in Figure 1a.

At radio wavelengths, ATCA observations have shown a shell-like remnant (Gaensler et al. 1997) that first appeared about 1300 days after explosion and has been brightening and expanding steadily ever since (Manchester et al. 2000). An image made on 9 September 1999 is shown in Figure 1b. The remnant has an irregular ring structure peaking just inside the optical inner ring, with an eastern lobe about twice as bright as the western lobe. The radio emission fills the inner ring.

SN1987A was first detected in the soft X-ray band in Feb 1991 (1448 days after the explosion) by the *ROSAT* satellite, and has been brightening steadily since then (Hasinger, Aschenbach, & Trümper 1996). With only 318 photons and the limited energy resolution of the *ROSAT* PSPC, Hasinger *et al.* were unable to distinguish between simple continuum models and more complex thermal plasma models of the spectrum.

We present the first *Chandra* images and spectra of SN1987A. Although the statistics are limited for these observations, we have resolved the remnant in X-rays and have obtained a high resolution spectrum that is dominated by thermal emission from highly ionized lines characteristic of temperatures above 10⁷ K. The luminosity has increased by a factor of three since 1995, but there is no evidence yet for an embedded point source.

2. IMAGE ANALYSIS

We have observed SN1987A twice with the Chandra X-ray Observatory (Weisskopf, O'Dell, & van Speybroeck 1996) as part of the Chandra Guaranteed Time Observations (GTO) program (Figure 1c and 1d). Chandra has unprecedented angular resolution (0.5 arcseconds HPD) in the X-ray band. It has two focal plane cameras and two sets of transmission gratings that can be inserted into the optical path. Our observations utilized the Advanced CCD Imaging Spectrometer (ACIS; Garmire et al. 2000), which takes high-resolution images with moderate non-dispersive energy resolution, and which can also serve as a readout device for the transmission gratings. Our first observation was made on 6 October 1999 using the High Energy Transmission Grating and the ACIS-S detector array. The 120 ks observation produced an undispersed zero-order image of the remnant with moderate energy resolution, and a set of dispersed spectra with high energy resolution. The second observation, made on 17 January 2000, used the ACIS S3 detector, and provided 10.7 ks of data with moderate nondispersive energy resolution.

The data were processed and filtered to reduce the background. We restricted photon energies to 0.3 - 8 keV and used ASCA grade 02346 events. In order to obtain the highest possible spatial resolution, we turned off the pixel randomization introduced by the standard data processing system¹. The light curves were examined for times of high background that could contaminate our results, but none were found. The first observation contained 696 photons meeting our criteria in the zero-order image, while the second observation had 583 photons. The astrometry of the raw images was adjusted by hand to agree with

¹The pipeline software adds a random offset of between $\pm \frac{1}{2}$ pixel to the sky position of each photon to prevent the appearance of Moiré patterns in *Chandra* images. This is unnecessary for long *Chandra* observations, because the spacecraft dither accomplishes the same thing.

the reference system of Reynolds et al. (1995), who determined a position of (05:35:27.97, -69:16:11.09) for SN1987A based on Hipparcos and VLBI data.

The optical and radio remnants measure roughly $1.7'' \times 1.2''$ on the sky, as do the raw X-ray images. This is barely resolved by the *Chandra*/ACIS instrument, which samples the $\sim 0.5''$ telescope image with 0.492'' detector pixels. Because *Chandra* moves slowly across the sky during each observation, the placement of ACIS detector pixels on the sky is not fixed during an observation, allowing us to deconvolve our data to obtain higher resolution. The ACIS data were binned into 0.125 arcsecond sky pixels (with the center of the CCD pixel projected into the corresponding sky pixel), and the resulting images were then deconvolved with a Maximum Likelihood algorithm (20 iterations; Richardson 1972; Lucy 1974), using an on-axis point spread function obtained with the MARX ray tracing software package. Smoothed versions of the deconvolved images are shown in Figure 1c and 1d, and have an effective resolution of about 0.3 arcseconds (FWHM). The X-ray remnant size, measured between peaks of the shell, is 1.2×1.0 arcseconds.

The SNR is generally shell-like, with the X-ray emission peaking just inside the optical inner ring, as expected on the basis of current models (Chevalier & Dwarkadas 1995; Borkowski, Blondin, & McCray 1997a). The X-ray emission is brightest in the eastern quadrant, where the new hot spots are appearing. We believe that the observed X-ray emission comes primarily from the shocked supernova debris and shocked circumstellar gas in a shell between the reverse shock and the blast wave (Borkowski, Blondin, & McCray 1997a). The blast wave is propagating with velocity $\sim 4,000$ km/s into a relatively low density ($n \sim 10^2$ cm⁻³) HII region. The presence of the reverse shock is indicated by spectroscopic observations made with HST/STIS, which show high velocity Ly α and H α emission coming from a surface interior to the circumstellar ring where the freely expanding supernova debris is suddenly slowed from $\sim 15,000$ km/s to $\sim 3,000$ km/s (Michael et al.

1998). The nonthermal radio emission probably comes from relativistic particles in the same zone.

The X-ray images in Figure 1 are overlaid with contours of the HST H α emission. Some of the X-ray hot spots agree well with optical hot spot positions (small differences of order 0.1 arcseconds are not significant); others do not. Differences between the two X-ray observations are probably dominated by statistical variations; a 1σ variation in these images corresponds to about 50 counts, or about 8% of the total, whereas the details of the deconvolved images typically involve fewer counts than that. Longer observations planned for Cycle 2 will provide images with greatly improved statistics.

Are we observing X-rays from the optical hot spots themselves? The evidence on this question is tantalizing but ambiguous. The X-ray images exhibit peaks in the general vicinity of the optical hot spots, but the positional agreement is not perfect; further, some of this structure is similar to that seen in the ATCA images, which does not seem to be related to the optical hot spots. STIS spectra of Spot 1 show line broadening consistent with shock velocities in the range 100 - 300 km/s (Michael et al. 2000). Shocks with such velocities produce X-rays with spectra much softer than the observed spectrum, and shock models with parameters chosen to fit observations of UV emission lines from Spot 1 predict X-ray fluxes only $\sim 0.5\%$ of the total X-ray flux observed by Chandra. On the other hand, a greater flux of X-rays may be emitted by faster (> 300 km/s) shocks that are also propagating into the hot spots. The X-ray emitting gas behind such shocks may not have had time to cool by radiation and emit observable optical and UV emission lines.

We see no evidence for a point source of X-rays in the interior of SN1987A. We have performed a Monte Carlo simulation to estimate our point source sensitivity. In this simulation, we added a point source (convolved with the PSF, with photon statistics) to the observed photon image in eighth-arcsecond pixels, rebinned to half-arcsecond pixels,

and compared the result to the original image using a χ^2 test. The 90% confidence limit on a central point source is 15% of the total SNR flux. This allows us to place an upper limit of 2.3×10^{34} ergs/s on the luminosity of any central point source (0.5 - 2 keV). This limit is not surprising in view of calculations showing that the debris should still be opaque to soft X-rays (Fransson & Chevalier 1987). (By comparison, Suntzeff *et al.* 1992 set an upper limit of 8×10^{36} erg/s on the contribution of a compact central source to the optical light curve on day 1500.)

3. LIGHT CURVE

The long-term light curve of SN1987A in soft X-rays is shown in Figure 2, where we have plotted observed fluxes (0.5 - 2.0 keV) calculated from our new observations together with earlier ROSAT measurements (Hasinger, Aschenbach, & Trümper 1996). ACIS count rates were converted to observed fluxes and source luminosities by fitting the undispersed spectra to plane parallel shock models. The ROSAT count rates were converted to observed fluxes using the same models that fit the ACIS data. The X-ray flux continues to increase monotonically, and is now substantially higher than the linear trend of the ROSAT data. This may be due to the interaction of the blast wave with parts of the equatorial ring, or may simply reflect higher densities in the regions now being shocked. The fact that both the X-ray and radio light curves continue to increase monotonically, combined with the morphological similarity of the X-ray and radio images, supports the notion that the shocks responsible for the X-ray emission are also responsible for accelerating the relativistic electrons that emit the radio waves (Chevalier & Dwarkadas 1995). The X-ray luminosity in Jan 2000 was 1.5×10^{35} ergs/s (0.5-2.0 keV), or 1.9×10^{35} ergs/s (0.5-10 keV), for a distance of 50 kpc.

4. DISPERSED SPECTRUM

Our first observation produced a dispersed high resolution spectrum, which is shown in Figure 3. X-ray events with inferred energy corresponding to their position along the dispersed spectrum were extracted using a 3 arcsecond wide source region, with 7.5 arcsecond background regions on either side, to optimize the signal to noise ratio. Photons from the positive and negative first orders of both the MEG and HEG were combined to produce the spectrum shown in Figure 3.

The spectrum is dominated by bright lines from the Helium-like and Hydrogen-like ionization stages of O, Ne, Mg, and Si. Preliminary fits to plane parallel shock models with constant electron temperature (vpshock in XSPEC V11) and abundances appropriate for the inner circumstellar ring (Lundqvist & Fransson 1996) and the LMC (Russell & Dopita 1992; Hughes, Hayashi, & Koyama 1998) give electron temperatures of $kT \approx 3$ keV and ionization timescales of $nt \approx 7 \times 10^{10}$ cm⁻³ s. This electron temperature is much lower than the post-shock proton temperature for a 4000 km s⁻¹ shock ($T_p \approx 30$ keV) because the time for temperature equilibration through Coulomb interactions is of order 5000 years. The shock ionization timescale, nt, is just about what would be expected for a blast wave that has propagated for $t \sim 6$ years into a gas having pre-shock density $n \sim 10^2$ cm⁻³.

The X-ray line shapes are determined by a combination of thermal and bulk motion of the rapidly expanding young remnant, and can be used to constrain the shock velocity and possibly its geometry. We have co-added four of the brightest isolated X-ray lines to examine the line profile. Preliminary analysis of this profile appears to be consistent with an equatorially brightened shell expanding with velocity ~ 4000 km/s, plus emission from lower velocity shocks entering the hotspots. We defer detailed discussion to a future paper on spectroscopic analysis of these data.

5. CONCLUSIONS

The Chandra X-ray Observatory has opened up an exciting new era of high spatial and spectral resolution X-ray astronomy. Our preliminary analysis demonstrates that the X-ray emission from SN1987A is beginning to show the effects of the interaction of the blast wave with the circumstellar medium, signalling the birth of a supernova remnant. For the first time, we can follow the development of a young supernova remnant (SNR) and confront theoretical models of SNR evolution with detailed X-ray observations.

SN1987A is a rapidly evolving object: the flux has increased by a factor of 3 in the past five years, and is expected to increase more dramatically in the near future. We predict that emission from hot spots, which now accounts for perhaps 20% of the X-ray flux, will dominate the X-ray flux within 2-3 years. The rapid timescale of changes requires periodic monitoring of SN1987A, using Chandra/ACIS to produce images of the remnant, XMM-Newton to produce high-resolution spectra, and HST to monitor the optical and UV images and spectra of the hot spots.

This work was supported by NASA contract NAS8-38252 and NASA grant NGT5-80. Support was also provided by NASA through grant GO-08243 from the Space Telescope Science Institute, which is operated by the Association of Universities for Research in Astronomy, Inc., under NASA contract NAS5-26555. We are grateful to Bryan Gaensler and to Peter Challis and the SINS team for providing their data for comparison with our *Chandra* observations, and to the HETG team at MIT for assistance with the analysis of the dispersed spectrum. The superb performance of the *Chandra* observatory is the result of years of work by thousands of scientists, engineers, and managers, and we are deeply indebted to their efforts. Finally, we acknowledge the very useful comments of our referee, which resulted in significant improvements to this paper.

References

Andreani, P., Ferlet, R., & Vidal-Madjar, A. 1987, Nature, 326, 770

Borkowski, K. J., Blondin, J. M., & McCray, R. 1997a, ApJ, 476, L31

Borkowski, K. J., Blondin, J. M., & McCray, R. 1997b, ApJ, 477, 281

Bouchet, P. et al. 2000, IAU Circ., 7354

Burrows, C. J., et al. 1995, ApJ, 452, 680

Chevalier, R. A., & Dwarkadas, V. V. 1995, ApJ, 452, L45

Fransson, C., & Chevalier, R. A. 1987, ApJ, 322, L15

Gaensler, B., et al. 1997, ApJ, 479, 845

Garmire, G. P., et al. 2000, ApJS, in preparation

Garnavich, P., Kirshner, R., & Challis, P. 2000, IAU Circ., 7360

Garnavich, P., et al. 2000, ApJ, submitted

Hasinger, G., Aschenbach, B., & Trümper, J. 1996, A&A, 312, L9

Hughes, J. P., Hayashi, I., & Koyama, K. 1998, ApJ, 505, 732

Kirshner, R. P., et al. 1987, ApJ, 320, 602

Koshiba, M., et al. 1987, IAU Circ., 4338

Lawrence, S., Sugarman, B., Bouchet, P., Crotts, A., Ugleshich, R., & Heathcote, S. 2000, ApJ, in press

Lucy, L. B. 1974, AJ, 79, 745

Lundqvist, P. & Fransson, C. 1996, ApJ, 464, 924

Luo, D., McCray, R., & Slavin, J. 1994, ApJ, 430, 264

Manchester, R., et al. 2000, PASA, in press

Maran, S., Pun, C. S. J., & Sonneborn, G. 2000, IAU Circ., 7359

Michael, E., et al. 1998, ApJ, 509, L117

Michael, E., et al. 2000, ApJ, submitted

Reynolds, J. E., et al. 1995, A&A, 304, 116

Richardson, W. H. 1972, J. Opt. Soc. Am., 62, 55

Russell, S. C., & Dopita, M. A. 1992, ApJ, 384, 508

Sonneborn, G., Altner, B., & Kirshner, R. P. 1987, ApJ, 323, L35

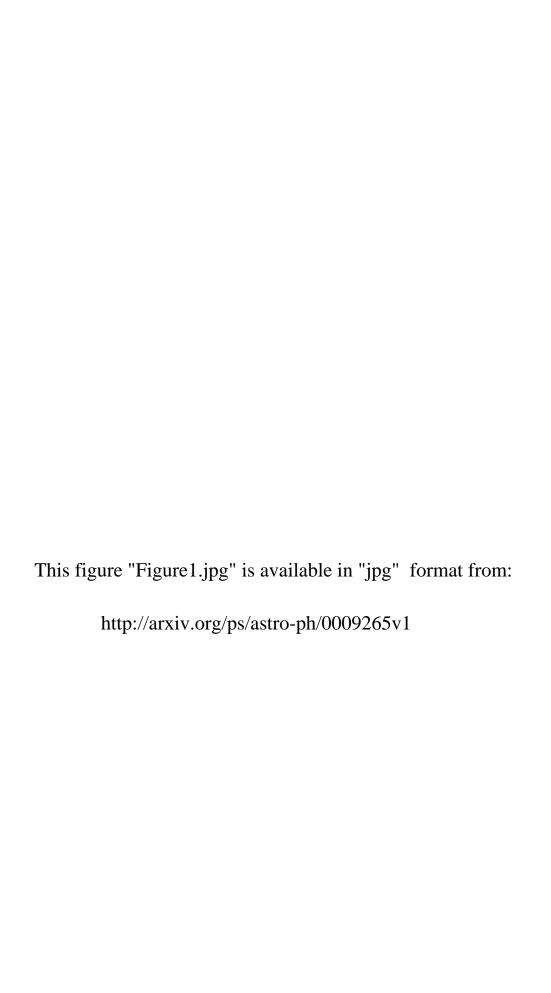
Suntzeff, N. B., et al. 1992, ApJ, 384, L33

Weisskopf, M. C., O'Dell, S. L., & van Speybroeck, L. P. 1996, Proc. SPIE, $2805,\,2$

Fig. 1.— Four recent images of SN1987A: a: HST image (log scaling) taken on 2 February 2000 (P. Garnavich, R. Kirshner, & P. Challis and the SINS team); b: Deconvolved ATCA 8 GHz image (square-root scaling) from 9 September 1999 (Manchester et al. 2000); c: Deconvolved ACIS image (linear scaling) from 6 October; d: Deconvolved ACIS image (linear scaling) from 17 January 2000. The images were made with identical pixel size and orientation (north is up). Contour overlays in panels b, c, and d are the optical ring from panel a. The ATCA data were kindly made available to us for this comparison by Bryan Gaensler and Dick Manchester. The Australia Telescope Compact Array is funded by the Commonwealth of Australia for operation as a National Facility managed by CSIRO.

Fig. 2.— SN1987A light curves in the 4.7 GHz (top) and soft X-ray (bottom) bands. The X-ray light curves are for the observed fluxes in the 0.5 - 2.0 keV band. The solid lines are the best-fit linear trends, fitted to the entire ATCA and ROSAT data sets.

Fig. 3.— Dispersed X-ray spectrum of SN1987A from the $\pm 1^{\rm st}$ orders of the MEG and HEG spectra. The spectrum has been smoothed with a Gaussian having FWHM = 0.03 keV.



This figure "Figure2.jpg" is available in "jpg" format from: http://arxiv.org/ps/astro-ph/0009265v1

